PHYSICAL REVIEW A **75**, 040301(R) (2007)

Fast quantum state control of a single trapped neutral atom

M. P. A. Jones, J. Beugnon, A. Gaëtan, J. Zhang,* G. Messin, A. Browaeys, and P. Grangier
Laboratoire Charles Fabry de l'Institut d'Optique (UMR 8501), Campus Polytechnique, RD 128, 91127 Palaiseau Cedex, France
(Received 18 September 2006; published 11 April 2007)

We demonstrate the initialization, readout, and high-speed manipulation of a qubit stored in a single ^{87}Rb atom trapped in a submicrometer-sized optical tweezer. Single-qubit rotations are performed on a time scale below 100 ns using two-photon Raman transitions. Using the spin-echo technique, we measure an irreversible dephasing time of 34 ms. The readout of the single atom qubit is at the quantum projection noise limit when averaging up to 1000 individual events.

DOI: 10.1103/PhysRevA.75.040301 PACS number(s): 03.67.Lx, 32.80.Pj, 42.50.Ct

The building block of a quantum computer is a qubit—an isolated two-level quantum system on which one can perform arbitrary single-qubit unitary operations. In the circuit approach to quantum computing [1], single-qubit operations are sequentially combined with two-qubit gates to generate entanglement and realize arbitrary quantum logic operations. In the alternative one-way quantum computing scheme [2], the ensemble of qubits is prepared in a highly entangled cluster state, and computations are performed using single-qubit operations and measurements. A wide range of physical systems are under investigation as potential qubits [1,3,4], including trapped single neutral atoms. In particular, the hyperfine ground states of alkali-metal atoms can be used to make qubits that are readily manipulated using microwave radiation or Raman transitions, with negligible decoherence from spontaneous emission. The usefulness of these techniques has been demonstrated with the realization of a five-qubit quantum register based on microwave addressing of single atoms trapped in an optical lattice [5]. A quantum register could also be formed using arrays of optical tweezers [6], each containing a single atom [7], with each site optically addressed using tightly focused Raman beams [8]. Several detailed proposals for performing two-qubit operations in such a tweezer array have been made, based on controlled collisions [9], dipole-dipole interactions between Rydberg atoms [10,11], and cavity-mediated photon exchange [12]. Alternatively, two-qubit operations could be performed without interactions by using photon emission [13] and quantum interference effects [14]. The recent observations of atom-photon entanglement [15,16] and two-photon interference between single photons emitted by a pair of trapped atoms [17,18] are major steps in this direction.

In this paper we describe how a single ^{87}Rb atom trapped in an optical tweezer can be used to store, manipulate, and measure a quantum bit. The qubit basis states are the $|0\rangle = |F=1, m_F=0\rangle$ and $|1\rangle = |F=2, m_F=0\rangle$ ground-state hyperfine sublevels (Fig. 1). We initialize the system by preparing the atom in the $|0\rangle$ state using optical pumping. Single-qubit operations are performed using two-photon Raman transitions. An unusual feature of our experiment is that we use the tightly focused optical tweezer as one of the Raman beams. In this way we obtain a Rabi frequency of $\Omega = 2\pi \times 6.7$ MHz with laser beams detuned by more than 10^6 linewidths from the nearest atomic transition. We perform a measurement of the state ($|0\rangle$ or $|1\rangle$) of each single atom with near unit efficiency, allowing us to perform projection-noise-limited measurements of the qubit state. Using Ramsey spectroscopy, we measure a dephasing time of 370 μs. This dephasing can be reversed using the spin-echo technique. In this way we have measured an irreversible dephasing time of 34 ms, which is almost six orders of magnitude longer than the time required to perform a π rotation. Due to the very large Rabi frequency, this ratio can approach the state of the art achieved in ion trap systems that have much longer coherence times [19].

We isolate and trap single ^{87}Rb atoms in an optical dipole trap created by a tightly focused far-off-resonant laser beam [20]. A custom-made objective lens with a numerical aper-

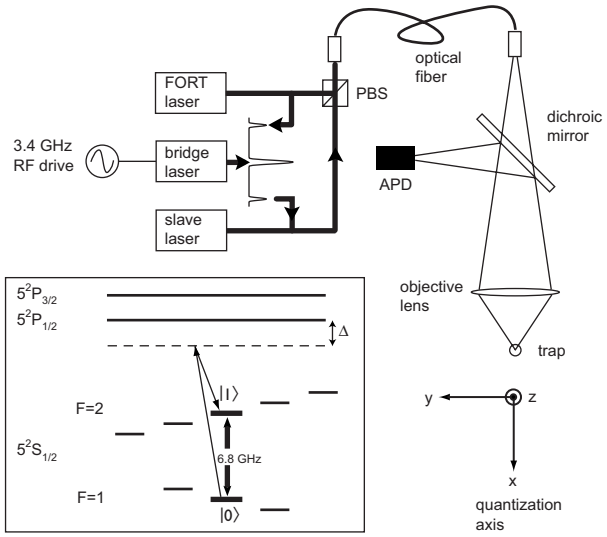

FIG. 1. Experimental setup. A high-performance objective lens creates a tightly focused optical dipole trap, which also acts as one of the Raman beams. The second Raman beam is generated using two additional diode lasers, and is superimposed with the trapping beam on a polarizing beam splitter (PBS). A single polarization-maintaining fiber carries both beams to the experiment. Inset: relevant energy levels of ^{87}Rb. The quantization axis is defined by a 0.36 mT magnetic field along the x axis.

*Present address: Key Laboratory of Quantum Optics, Ministry of Education—PRC and Institute of Opto-Electronics, Shanxi University, China.

ture of 0.7 is used to focus the beam at 810 nm to a diffraction-limited waist of $\approx 0.9\ \mu$m. With a power of 0.95 mW we obtain a trap at the focus with a depth of 1.2 mK and oscillation frequencies of 125 and 23 kHz in the radial and axial directions, respectively. The trap is loaded from an optical molasses. A "collisional blockade" effect forces the number of atoms in the trap to be either zero or one. We measure the initial temperature of the atom to be 90 μK. The trap lifetime in the absence of any near-resonant light is 3 s and the heating rate is $0.021 \pm 0.005\ \mu\text{K ms}^{-1}$.

The presence of an atom in the trap is detected using its fluorescence from the molasses cooling light. As shown in Fig. 1, the fluorescence is collected by the same objective used to make the optical dipole trap, and is separated off using a dichroic mirror before being imaged onto an avalanche photodiode. When an atom is present in the trap we detect $\approx 10\,000$ photons s^{-1}, compared to a typical background count rate of 2000 s^{-1} for an empty trap. By setting a threshold value for the fluorescence we can unambiguously detect the presence of an atom within ≈ 15 ms of its arrival. This signal is then used to shut off the molasses light and trigger the experimental sequence.

Once a single atom has been detected in the trap, it is prepared in the logical state $|0\rangle$ using optical pumping on the $D2$ line. For this we use a π-polarized Zeeman pumping beam resonant with the $F=1 \rightarrow F'=1$ transition and a hyperfine repumping beam resonant with the $F=2 \rightarrow F'=2$ transition. The quantization axis is defined by a 0.36 mT magnetic field along the x axis. After 200 μs of optical pumping the atom is prepared in the logical state $|0\rangle$ with 85% efficiency. We have determined that all of the atoms not prepared in $|0\rangle$ are left in the other $F=1$ sublevels. These atoms are not affected by the Raman beams due to the Zeeman shift.

We perform single-qubit rotations by coupling the logical states $|0\rangle$ and $|1\rangle$ using a two-photon stimulated Raman transition. Driving the Raman transition requires two phase-locked laser beams separated by the hyperfine transition frequency $\omega_{\text{hf}}/2\pi \simeq 6.8$ GHz. In our experiment, the optical dipole trap forms one of these beams. The trapping light is produced using a grating-stabilized external cavity diode laser. To generate the second Raman beam we use two additional 810 nm diode lasers as shown in Fig. 1. The frequency offset is obtained by modulating the current of the bridge laser at 3.4 GHz, adding two sidebands to its output with the desired frequency separation. The bridge laser is phase locked to the dipole trap laser by injection locking on one of the sidebands [21]. A Mach-Zender interferometer is used to remove 90% of the carrier power from the output of the bridge laser, which is then used to injection lock a third slave laser tuned to the other sideband. An acousto-optic modulator allows intensity control of the Raman beam as well as fine tuning of the frequency difference between the two beams. The two beams are sent to the experiment through the same polarization-maintaining optical fiber. The optical dipole trap and the Raman beam have orthogonal linear polarizations in the z-y plane in order to drive $\Delta m_F = 0$ transitions.

After the Raman beams have been applied, we measure the state ($|0\rangle$ or $|1\rangle$) of the atom. A probe laser beam resonant with the $5\ ^2S_{1/2}F=2 \rightarrow 5\ ^2P_{3/2}F'=3$ cycling transition is used to state-selectively push atoms in state $|1\rangle$ out of the trap by radiation pressure. During the 100 μs that the probe beam is applied, the depth of the trap is lowered to 0.4 mK to make sure that atoms in $|1\rangle$ are rapidly removed from the trap before they can be pumped into the $F=1$ hyperfine level by off-resonant excitation. Atoms that are initially in state $|0\rangle$ are unaffected by this procedure and remain in the trap [22]. We then turn on the molasses cooling light for 10 ms and determine whether or not the atom is still in the trap. The states $|0\rangle$ and $|1\rangle$ are therefore mapped onto the presence (absence) of the atom at the end of the sequence, as was shown in similar experiments with cesium atoms [5,23].

This technique actually measures whether the atom is in the $F=1$ or $F=2$ hyperfine level at the end of the sequence. Therefore, atoms that are left in the $F=1, m_F=\pm 1$ sublevels after optical pumping also contribute to the signal, leading to a 15% background on the probability that the atom remains after the push-out laser is applied. To independently check how accurately we can determine whether an atom is in the $F=1$ or $F=2$ hyperfine state, we prepare the atom in either $F=1$ or $F=2$ by blocking one of the optical pumping beams. We measure that the probability that we have incorrectly assigned the hyperfine level of the atom at the end of a single sequence is less than 2%.

At the end of a single-qubit operation, the qubit is in general in a superposition $\alpha|0\rangle + \beta|1\rangle$. In order to measure the coefficients α and β we repeat each experiment (trapping, preparation, qubit operation, and readout) 100 times under identical conditions. In the absence of technical noise, the statistical error on the mean recapture probability after N identical experiments should be given by the standard deviation of the binomial distribution $\sigma = \sqrt{p(1-p)/N}$ where p is the probability that the atom is in $F=1$. We have checked experimentally that this is the case for values of p between 0.005 and 0.95, and for N up to 1000. Our measurements of the coefficients α and β are therefore limited solely by quantum projection noise.

The combined performance of these techniques was investigated by performing Rabi rotations between the states $|0\rangle$ and $|1\rangle$. The results for two different Raman beam intensities are shown in Fig. 2. At our maximum intensity, we reach a Rabi frequency of $\Omega = 2\pi \times 6.7$ MHz, which corresponds to a $\pi/2$ rotation time of 37 ns. The 15% background is due to the imperfect optical pumping discussed above. At both high and low power the oscillations are strongly damped, decaying after approximately five complete periods. We attribute this damping to intensity fluctations in the Raman beams, due both to technical intensity noise (we measure $\approx 2\%$ rms on each beam), and to the time-varying intensity experienced by the atom due to its motion. The latter is modeled by averaging the Rabi frequency over the motion of the atom, assumed to be thermal [23]. The solid lines in Figs. 2(a) and 2(b) are fits using a model that includes both effects. For both curves the temperature is fixed at 90 μK and the total technical intensity noise (both beams) is fixed at 2.5%. The initial contrast and the Rabi frequency are the only adjustable parameters. The model is in good agreement for both curves, despite the 130 000-fold reduction in the Raman beam intensity (using neutral density filters) between the two curves.

We have also investigated the coherence properties of this

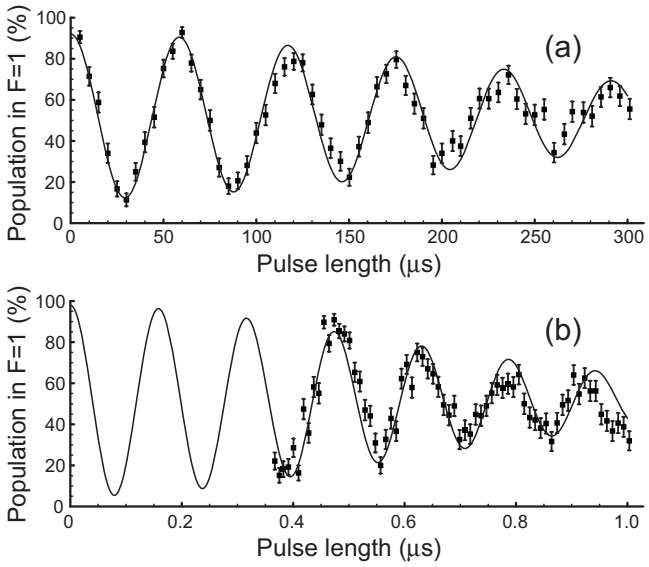

FIG. 2. Single-atom Rabi oscillations. We measure the fraction of atoms in $F=1$ as a function of the Raman pulse length, at low (a) and high (b) intensity. We observe damped Rabi oscillations between the two qubit states with Rabi frequencies of $\Omega=2\pi\times 18$ kHz (a) and $\Omega=2\pi\times 6.7$ MHz (b). In (b) we could not observe the first 400 ns due to the response time of the acousto-optic modulator. The error bars correspond to the quantum projection noise.

qubit using Ramsey spectroscopy. We apply two $\pi/2$ pulses separated by a variable time t, with a fixed value of the Raman detuning δ. In the limit $\delta\tau\ll 1$ where τ is the $\pi/2$ pulse length, the population measured in the $|1\rangle$ state varies as $P(t)=\cos^2(\delta t/2)$. The results of this measurement with $\tau=1.2$ μs and $\delta=2\pi\times 20.8$ kHz are shown in Fig. 3. The contrast of the interference fringes decays as the time between the two $\pi/2$ pulses is increased, with a $1/e$ decay time of approximately 370 μs due to dephasing of the atomic qubit compared to the Raman beams. The dephasing mechanisms that operate in optical dipole traps have been extensively studied [23]. In our case, the dominant dephasing mechanism

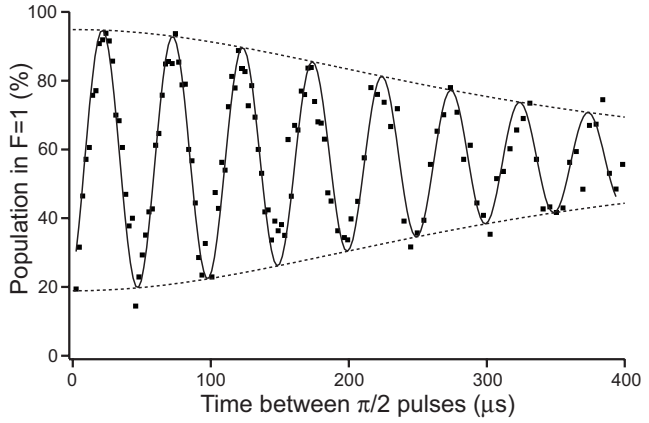

FIG. 3. Ramsey fringes recorded with a $\pi/2$ pulse length of 1.2 μs and a detuning $\delta=2\pi\times 20.8$ kHz. The solid line is a fit using the model presented in [23], which yields a dephasing time $T_2^*=370$ μs. The dotted line is the envelope of this fit.

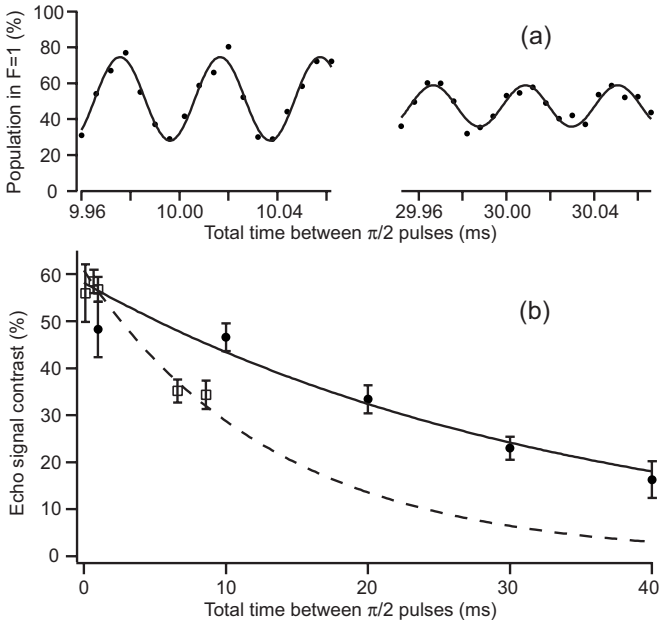

FIG. 4. (a) Example of the echo signal. We fix the time between the first $\pi/2$ pulse and the π pulse at $T=5$ (left) and 15 ms (right), and vary the time of the second $\pi/2$ pulse around $t=2T$. The trap depth is $U=0.4$ mK, and the magnetic field is $B=0.18$ mT. (b) Echo signal contrast as a function of the total time between the $\pi/2$ pulses with $U=1.2$ mK and $B=0.36$ mT (open squares) and $U=0.4$ mK and $B=0.18$ mT (filled circles). The dashed and solid lines are exponential fits with $1/e$ decay times of 13 ± 2 and 34 ± 5 ms, respectively.

arises from the finite temperature of the atoms in the trap. Due to the 6.8 GHz hyperfine splitting, the detuning of the dipole trap Δ is slightly different for the $|0\rangle$ and $|1\rangle$ states, which therefore experience slightly different ac Stark shifts. This gives rise to a position dependence of the qubit transition frequency $\omega(\mathbf{r})=\omega_{\mathrm{hf}}+\eta U(\mathbf{r})/\hbar$, where the differential ac Stark shift coefficient $\eta(\approx\omega_{\mathrm{hf}}/\Delta)=7\times 10^{-4}$ for our trap. Averaged over the motion of the atom in the trap, this effect shifts the detuning δ between the atomic resonance and the Raman beams by an amount which is different for each atom in a thermal ensemble, depending on its energy. As shown in [23], this gives rise to a decay of the contrast with a characteristic $(1/e)$ decay time $T_2^*=1.94\hbar/\eta k_B T$. We measure a dephasing time of $T_2^*=370$ μs, which is longer than the theoretical value $T_2^*=220$ μs that we would expect at 90 μK. By varying the temperature we have confirmed that the dephasing is due to the motion of the atom, although this quantitative disagreement remains unexplained.

The dephasing due to the motion of the atoms in the trap can be reversed using the spin-echo technique [23,24]. An additional population-inverting π pulse applied midway between the two $\pi/2$ pulses ensures that the phase accumulated during the second period of free evolution is the opposite of that acquired during the first. The echo signals that we obtain are shown in Fig. 4. The echo signal decays due to the decay of the populations (T_1 processes) and the loss of atoms to other Zeeman states, as well as irreversible dephasing caused by fluctuations in the experimental parameters. To illustrate this, we repeated the spin echo experiments with a reduced

trap depth and a smaller magnetic field. Lowering the trap depth reduces the rate of hyperfine mixing due to spontaneous Raman transitions induced by the optical dipole trap, and reducing the magnetic field reduces the sensitivity of the qubit states to ambient magnetic field fluctuations. As shown in Fig. 4, this resulted in a significant increase in the decay time of the echo signal from 13 to 34 ms.

In conclusion, we have demonstrated that a single rubidium atom trapped at the focal point of a large-numerical-aperture lens is a promising system for encoding a qubit. With improved state preparation and the elimination of technical intensity noise, the fidelity of our single qubit operations will ultimately be limited by the motion of the atom. This effect could be reduced by further laser cooling. As well as their importance for high-speed quantum logic, fast single-qubit operations are also important in many entanglement schemes. Most existing protocols require atoms initialized in $|0\rangle$ to be rotated into a superposition state before the entanglement operation is applied [11,25]. Several proposals for generating entanglement using photon emission also require state rotation between successive photons [25,26]. In our experiment, we can generate single photons at a rate of 5 MHz [17], leaving just 200 ns between successive photon emission events in which to perform a qubit rotation. Here we show that we can perform single-qubit rotations on this time scale, and thus avoid limiting the rate at which entangled pairs can be created and gate operations performed in our system.

This work was supported by Institut Francilien de Recherche sur les Atomes Froids (IFRAF), ARDA/DTO, and the Integrated Project SCALA from the European IST/FET/QIPC program. M.P.A.J. was supported by the EU Marie Curie Grant No. MEIF-CT-2004-009819. We thank the laser cooling group at NIST Gaithersburg, Poul Jessen, Ivan Deutsch, and Gerhard Birkl for helpful discussions.

[1] M. A. Nielsen and I. L. Chuang, *Quantum Computation and Quantum Information* (Cambridge University Press, Cambridge, U.K., 2000).
[2] R. Raussendorf and H. J. Briegel, Phys. Rev. Lett. **86**, 5188 (2001).
[3] *Quantum Computing and Quantum Bits in Mesoscopic Systems*, edited by A. Leggett, B. Ruggiero, and P. Silvestrini, eds., (Springer, Berlin, 2004).
[4] D. Liebfried, R. Blatt, C. Monroe, and D. Wineland, Rev. Mod. Phys. **75**, 281 (2003).
[5] D. Schrader *et al.*, Phys. Rev. Lett. **93**, 150501 (2004).
[6] R. Dumke *et al.*, Phys. Rev. Lett. **89**, 097903 (2002).
[7] S. Bergamini *et al.*, J. Opt. Soc. Am. B **21**, 1889 (2004).
[8] D. D. Yavuz *et al.*, Phys. Rev. Lett. **96**, 063001 (2006).
[9] U. Dorner *et al.*, J. Opt. B: Quantum Semiclassical Opt. **7**, S341 (2006).
[10] I. E. Protsenko, G. Reymond, N. Schlosser, and P. Grangier, Phys. Rev. A **65**, 052301 (2002).
[11] M. Saffman and T. G. Walker, Phys. Rev. A **72**, 022347 (2005).
[12] L. You, X. X. Yi, and X. H. Su, Phys. Rev. A **67**, 032308 (2003).
[13] B. Darquié *et al.*, Science **309**, 454 (2005).
[14] L.-M. Duan *et al.*, Phys. Rev. A **73**, 062324 (2006).
[15] B. B. Blinov, D. L. Moehring, L.-M. Duan, and C. Monroe, Nature (London) **428**, 153 (2004).
[16] J. Volz *et al.*, Phys. Rev. Lett. **96**, 030404 (2006).
[17] J. Beugnon *et al.*, Nature (London) **440**, 779 (2006).
[18] P. Maunz *et al.*, e-print quant-ph/0608047.
[19] C. Langer *et al.*, Phys. Rev. Lett. **95**, 060502 (2005).
[20] N. Schlosser, G. Reymond, I. Protsenko, and P. Grangier, Nature (London) **411**, 1024 (2001).
[21] M. J. Snadden, R. B. M. Clarke, and E. Riis, Opt. Lett. **22**, 892 (1997).
[22] We observe a small (5%) loss due to the reduction in trap depth. This reduces the initial contrast in Fig. 2.
[23] S. Kuhr *et al.*, Phys. Rev. A **72**, 023406 (2003).
[24] M. F. Andersen, A. Kaplan, and N. Davidson, Phys. Rev. Lett. **90**, 023001 (2003).
[25] S. D. Barrett and P. Kok, Phys. Rev. A **71**, 060310(R) (2005).
[26] Y. L. Lim, A. Beige, and L. C. Kwek, Phys. Rev. Lett. **95**, 030505 (2005).